

# Dielectric Spectroscopy of a Stretched Polymer Glass: Heterogeneous Dynamics and Plasticity

Roberto Pérez-Aparicio,<sup>†</sup> Denis Cottinet,<sup>†</sup> Caroline Crauste-Thibierge,<sup>†</sup> Loïc Vanel,<sup>‡,§</sup> Paul Sotta,<sup>‡</sup> Jean-Yves Delannoy,<sup>‡</sup> Didier R. Long,<sup>\*,‡</sup> and Sergio Ciliberto<sup>\*,†</sup>

<sup>†</sup>Laboratoire de Physique de l'École Normale Supérieure, CNRS/Université de Lyon, UMR 5672, 46 allée d'Italie, 69007 Lyon, France

<sup>‡</sup>Laboratoire Polymères et Matériaux Avancés, CNRS/Rhodia-Solvay, UMR 5268, 85 avenue des Frères Perret, 69192 Saint Fons, Cedex, France

<sup>§</sup>Institut Lumière Matière, CNRS/Université Lyon 1, UMR 5306, 69622 Villeurbanne, France

**ABSTRACT:** We study the dielectric relaxation of polycarbonate (PC) at room temperature under imposed strain rate  $\dot{\gamma}$ , above the yield stress, and up to 13% strain. We find that the dielectric response of stretched PC behaves as if it was heated up at a temperature just below its glass transition temperature,  $T_g \approx 423$  K for PC. Indeed, in the frequency range of our experiment ( $10^{-2}$  and  $10^3$  Hz), the dielectric response of the stretched PC at room temperature superimposes to the dielectric response of PC at a temperature  $T_a(\dot{\gamma}) < T_g$ , which is a function of strain rate. Specifically we observe that at  $T_a$  the dominant relaxation time  $\tau_\alpha(T_a)$  of PC at rest is related to  $\dot{\gamma}$  in such a way that  $\tau_\alpha(T_a) \sim 1/\dot{\gamma}$  at and beyond the yield point. In our experiment,  $10^{-5} \text{ s}^{-1} < \dot{\gamma} < 10^{-3} \text{ s}^{-1}$ , the temperature shifts  $T_g - T_a$  are of a few kelvin. The mechanical rejuvenation modifies the dielectric response at frequencies smaller than 10 Hz, whereas for higher frequencies the spectrum is only slightly modified.

## 1. INTRODUCTION

A very important aspect of polymers is their remarkable mechanical properties which depend on their glass transition temperature ( $T_g$ ). At temperatures below  $T_g$  the elastic modulus of a polymer glass can be of the order of  $10^9$  Pa,<sup>1</sup> while it decreases down to about  $10^5$  Pa above  $T_g$ . Such mechanical properties are directly related to the dynamic processes at the molecular level which are characteristic of this kind of system. For this reason, the understanding of the dynamics at the molecular level is of the utmost importance, on one hand, for learning about the macroscopic features and, on the other hand, for the development of new interesting tailored polymers from the technological point of view.

Important efforts have been made in the past decades to understand the glass transition phenomenon. In this way polymer dynamics has been investigated extensively through various experimental techniques and theoretical approaches with the combination of computer simulation techniques.<sup>1-5</sup> At temperatures  $T \geq T_g$ , in the so-called supercooled liquid regime, the structural or  $\alpha$ -relaxation becomes active allowing the system to flow, yielding a significant decay in the dynamic modulus down to  $10^5$  Pa. The  $\alpha$ -relaxation is responsible for

the glass transition phenomenon allowing the rearrangements of the structure within the polymer. The associated length scale is the typical interchain<sup>6</sup> distance, and its characteristic time scale covers a wide range from nanoseconds to seconds—which implies the need of using a combination of techniques. One of the important features of the glass transition is the heterogeneous dynamics close to  $T_g$ ,<sup>7,8</sup> which has been demonstrated experimentally over the past years by different techniques: NMR,<sup>9-11</sup> fluorescence recovery after photo-bleaching (FRAP),<sup>12-16</sup> dielectric hole burning,<sup>17</sup> or solvation dynamics.<sup>18</sup> The characteristic size  $\xi$  of the dynamical heterogeneities has been estimated by NMR<sup>10</sup> to be 3–4 nm at  $T_g + 20$  K (in the case of van der Waals liquids), whereas it is as small as 1 nm in glycerol.<sup>11,19</sup>

Since mechanical features are directly related to the dynamic behavior, it is very important to investigate the structural relaxation during the polymer deformation below  $T_g$  where these materials present their particular properties. For example,

during a deformation experiment, a polymer glass presents a yield stress at strains of about 10% corresponding to a maximum peak in the stress–strain curve. Above yield there is a plateau at stress values lower than the yield peak where the polymer undergoes plastic flow. At even higher deformations, strain hardening can be observed for high molecular weight entangled or cross-linked polymers. These properties have been studied for many years due to their high importance for applications.<sup>20</sup> Some experimental results led to the concept of mechanical rejuvenation which has been highly debated.<sup>21,22</sup> In the present paper, it will only refer to a mechanically induced acceleration of the dynamics in contrast with the slowing down dynamics during aging.

The first model for describing plastic deformation has been the Eyring model, according to which free energy barriers are reduced under the applied stress. This effect is controlled by the so-called activation volume  $V^*$  which is an adjustable parameter without clear interpretation.<sup>23,24</sup> The change of molecular dynamics in polymer glasses under deformation is not well understood. Two possible scenarios can be envisioned: (i) homogeneous effect on the dynamics, the whole spectrum being shifted toward shorter times, or (ii) an inhomogeneous modification of the relaxation time distribution due e.g. to localization of the deformation on microscopic scales. This issue has been investigated experimentally by Loo et al.,<sup>25</sup> who studied the dynamics in the amorphous phase of polyamide under stress by NMR. Dynamics under stress has also been considered by Ediger et al.,<sup>26,27</sup> by measuring the diffusion coefficient of small molecular probes during stretching experiments, or by Lesser et al.,<sup>28</sup> by tensile experiments coupled with dielectric spectroscopy. They have proposed an explanation of the connection between dynamical heterogeneities and plastic behavior, indicating an enhanced mobility and a more homogeneous dynamics (in comparison to the unstrained system) during uniaxial extension. By considering the relaxation function of probes orientation, Ediger et al. have shown that the relaxation time spectrum under deformation is narrower as compared to the spectrum at rest.

Mechanical properties of glasses have been also studied by molecular dynamics (MD) simulations.<sup>29–35</sup> In particular, Leonforte et al.<sup>33</sup> and Riggleman et al.<sup>34,35</sup> have shown that mechanical properties are heterogeneous. When glasses are submitted to an applied strain, the deformation field is nonaffine. Riggleman et al. have shown that the elastic modulus is heterogeneous on a scale of order 1 nm, with some regions having negative moduli. The possible link between dynamical heterogeneities and these mechanical heterogeneities has been discussed by Dequidt et al.<sup>36</sup> The idea that stress enhances molecular mobility is supported by these simulations. This idea has also been considered by Chen and Schweizer within the nonlinear Langevin equation model (NLE).<sup>23,24,37–39</sup> Their model allowed to reproduce many features of plastic deformation. Though these studies support the notion that the dynamics is enhanced during plastic deformation, several of these approaches are mean field theories, which neglect the spatial description. Thus, a detailed analysis of the dynamical behavior at the molecular level during plastic deformation is still lacking.

Dielectric spectroscopy (DS) allows investigating the molecular dynamics of relaxation processes by means of the polarization of molecular dipoles on the polymer sample. This technique is directly sensitive to polymer mobility, and it can be used to quantify the mobile fraction of polymer. Thus, it is very

convenient for the study of the microscopic mechanisms of plasticity. It has already been used in combination with mechanical deformation by Lesser et al.<sup>28</sup> on PVC uniaxially stretched until yield stress. Although this work answers to several questions, it is not yet completely understood how molecular dynamics is affected during deformation, especially at low frequencies where the evolution of the structural relaxation can be observed during the plastic deformation.

In this article we propose an experimental setup composed of a uniaxial tensile device coupled with an innovative dielectric spectrometer<sup>40</sup> which allows the simultaneous measurements of the dielectric properties in a wide range, spanning at least 4 orders of magnitude in frequency. It gives us access to the full microscopic information at each “deformation state” during the whole uniaxial deformation. The experiments are performed using a well-studied polymer: polycarbonate (PC) glass<sup>41,42</sup> with a glass transition temperature  $T_g = 423$  K. The paper is organized as follows. In section 2, we describe the experimental setup which has been developed and which is based on a combination of uniaxial stretching and multifrequency dielectric measurements. Results are presented and discussed in section 3.

## 2. EXPERIMENTAL METHOD

**2.1. Experimental Setup.** Our experimental setup is composed of a homemade dielectric spectrometer coupled with a tensile machine for uniaxial deformation of films. The scheme of the experimental setup is presented in Figure 1. The designed device allows the

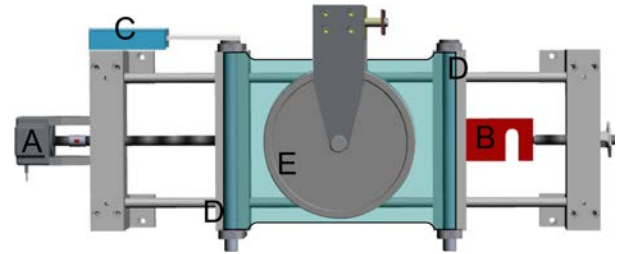


**Figure 1.** Experimental setup: motor (A), load cell (B), linear transducer (C), sample fastening cylinders (D), and electrodes for dielectric measurement (E).

investigation of polymer film samples of a maximum width of 210 mm. We used dog-bone-shape sheets in order to focus the deformation of the film between the electrodes for dielectric measurement, and we apply uniaxial strain up to 13% strain. The whole device was installed inside a Faraday cage in order to avoid electrical noise on the dielectric response signal from external sources. Measurements were performed at room temperature (no temperature control implemented). The room temperature was far below the glass transition (about  $T_g - 125$  K); thus, small temperature variations are negligible.

**2.2. Sample.** We investigated an extruded film MAKROPOL DE 1-1 000000 (from BAYER) based on Makrolon polycarbonate (PC) with a  $T_g$  of about 150 °C. The sample sheets had a thickness of 125  $\mu\text{m}$ . They are cut and used as received.

**2.3. Mechanical Deformation.** The mechanical part is composed of two cylinders (210 mm long, 16 mm of diameter) used to fasten the sample, a load cell of 2000 N capacity (Interface SM-2000N), a precision linear transducer to measure the position over a range of 100 mm (Vishay Series REC 115L), and a brushless servo motor with a coaxial reducer (Transtechnik MAC140-A1, maximum speed is 2000 rpm at 24 VDC). The experiments were done at constant strain rate until the stretch ratio  $\lambda$  is about 1.08 (8% strain), with  $\lambda = L/L_0$ ,  $L_0$  being the original length and  $L$  the new length after stretching. The maximum stress or yield stress was reached for  $\lambda = 1.06$ . We fixed four

different relative strain rates:  $2.5 \times 10^{-3}$ ,  $2.5 \times 10^{-4}$ ,  $2.5 \times 10^{-5}$ , and  $2.5 \times 10^{-6} \text{ s}^{-1}$ . The relative strain rate is denoted  $\dot{\gamma}$  and defined as

$$\dot{\gamma}(t) = \frac{d}{dt} \left( \frac{L(t) - L_0}{L_0} \right) = \frac{v(t)}{L_0} \quad (1)$$

where  $v(t)$  is the linear speed of the moving cylinder. The samples were dog-bone shaped, and the effective dimensions of the area under deformation were 200 mm in width and 230 mm in length. The deformation was performed at fixed strain rate.

**2.4. Dielectric Spectroscopy.** *2.4.1. Theoretical Background.* Dielectric spectroscopy allows the investigation of the dielectric response of a material as a function of frequency<sup>43</sup> by the interaction of an external field with the electric dipole moment of the sample, often expressed by the complex dielectric permittivity or dielectric constant:

$$\epsilon(\omega) = \frac{D(\omega)}{E(\omega)} \quad (2)$$

where  $D(\omega)$  is the dielectric displacement and  $E(\omega)$  the electric field, both dependent on the angular frequency  $\omega$ .  $\epsilon(\omega)$  has a complex magnitude  $\epsilon(\omega) = \epsilon'(\omega) - i\epsilon''(\omega)$ , with  $\epsilon'(\omega)$  the real component of permittivity which is related to the electrical energy stored by the sample and  $\epsilon''(\omega)$  the imaginary component of permittivity which indicates the energy losses. The loss tangent is

$$\tan \delta = \frac{\epsilon''(\omega)}{\epsilon'(\omega)} \quad (3)$$

where  $\delta$  is the phase shift between  $D(\omega)$  and  $E(\omega)$ .

If the electric dipole moments of the sample have a molecular origin, dielectric spectroscopy may give information on the molecular motions. It is a very convenient technique in the field of polymer physics<sup>2</sup> because it allows the investigation of the structural or  $\alpha$ -relaxation as well as more localized molecular motions (e.g.,  $\beta$ -relaxation). The measurement is directly sensitive to local molecular motion without any added molecular probes.

The different experimental techniques and procedures for dielectric spectroscopy depend on the frequency range of interest. At low and intermediate frequencies ( $10^{-3}$ – $10^7$  Hz) the parallel-plates capacitor is a good geometry. The sample is a dielectric insulator between two electrodes. The complex impedance  $Z(\omega)$  of this capacitor can be modeled by a resistance  $R(\omega)$  in parallel with a capacitance  $C(\omega)$ , and it can be expressed as

$$\frac{1}{Z(\omega)} = \frac{1}{R(\omega)} + iC(\omega)\omega \quad (4)$$

From  $R(\omega)$  and  $C(\omega)$  it is possible to calculate  $\epsilon'(\omega)$  and  $\epsilon''(\omega)$  as

$$\epsilon'(\omega) = \frac{C(\omega)d}{\epsilon_0 S} \quad (5)$$

$$\epsilon''(\omega) = \frac{d}{\epsilon_0 SR(\omega)\omega} \quad (6)$$

where  $d$  is the distance between the capacitance plates, equal to the thickness of the sample,  $S$  their surface, and  $\epsilon_0$  the vacuum permittivity.

The rheodielectric measurements on polymers in the vicinity of the glass transition are discussed in the review article by Watanabe et al.<sup>44</sup> It is important to notice that when studying dielectric response of materials, when they are at equilibrium, one may use the Green–Kubo theorem which relates the noise to the relaxation dynamics.<sup>45</sup> In this work, we measure the dielectric response, not the noise. Since our system is not at equilibrium, we restrict our work to frequencies much larger than  $1/t$  where  $t$  is the duration of the experiment, for which we may assume a quasi-static equilibrium.

*2.4.2. Dielectric Spectroscopy Setup.* In this article we used an innovative dielectric spectroscopy technique already presented in ref 40 which allows the simultaneous measurement of the dielectric properties in a 4 orders of magnitude frequency window chosen in the range of  $10^{-2}$ – $10^3$  Hz. It enables measuring resistances and

capacitances in the ranges  $R \leq 10^{12} \Omega$  and  $C > 10^{-11}$  F with a good accuracy. This multifrequency experiment is very useful in the study of transient phenomena such as polymer films deformation. Indeed, if each frequency has to be measured individually, the measurement is very long and has poor time resolution. In contrast, with the simultaneous multifrequency measurement, the acquisition duration is fixed by the lowest excitation frequency and higher frequencies come for free. The required time resolution will also limit the acquisition extension, and as a consequence it constrains the lowest frequency that can be effectively measured.

In our experiment the sample film was confined by two disc-shaped electrodes of 18 cm diameter (see Figure 1), which constitute the capacitance  $C$ . This capacitance was measured by the dielectric spectrometer composed of the dielectric electronics described in ref 40, a wave generator (Agilent 33500B Series), low noise batteries, and an acquisition card (National Instrument PXI-4472, 24 bits of resolution). Data acquisition was performed via a Labview homemade program and data treatment using Matlab.<sup>40</sup> During deformation, the PC film moves relatively to the electrodes. Thus, postbuckling deformation may appear (well-known in PC films), which could hinder the contact with electrodes. In order to ensure a good contact between the electrodes and the sample during the whole deformation experiment, we used an aqueous gel of contact (Drexco Medical Ref. 10904). The gel has very low electrical resistivity compared to the sample. It does not perturb the sample response because water absorption in PC films is only 0.2%. In any case, the possible influence of the gel on the measurement has been carefully checked. We first compared the dielectric spectra measured using the gel layers with the available data of  $\epsilon(\omega)$  of PC at various temperatures. We also measured the PC  $\epsilon(\omega)$  using standard aluminum electrodes glued on the sample surfaces by heating above  $T_g$ . In both cases no significant difference has been observed with respect to the measurements performed with the gel layer. In order to check for other possible artifacts introduced by the gel thin layer, we recently performed other measurements using oils charged with carbon. Within experimental errors no difference has been noticed between the results obtained with the gel and those obtained using mineral oils.

**2.5. Data Analysis.** As already mentioned, the acquisition time, the sample size, and the smallest resolved frequency are coupled. For example, in order to measure the dielectric response at the lowest frequency, i.e., 0.03125 Hz, we would need an acquisition window of 128 s (4 periods). Because our measurement were performed on a transient phenomenon (the deformation), the acquisition is constrained by the duration of this transient phenomenon. Moreover, we varied the strain rate. For example, at the highest strain rate,  $2.5 \times 10^{-3} \text{ s}^{-1}$ , the maximum deformation was reached within 26 s. In order to compare the experiments at various strain rates, we set the increment of deformation  $\lambda$  between successive data points ( $\sim 1\%$ ). For each strain rate this imposes the time window available for each data point, e.g.,  $\sim 2$  s at the strain rate  $2.5 \times 10^{-3} \text{ s}^{-1}$ . The time window determines the lowest frequency resolved at each strain rate, e.g., 1 Hz at the strain rate  $2.5 \times 10^{-3} \text{ s}^{-1}$ . The signal-to-noise ratio was increased a lot by considering a frequency slightly higher than this lowest measurable frequency because the time window enables then to average on a larger number of periods.

In our dielectric measurement, we had also to take into account the decrease in the sample thickness during uniaxial stretching. The effective surface of the capacitor may also vary due to contact gel flow around the electrodes during stretching. To overcome these geometric effects, two corrections can be safely applied on the data. On one hand, we focused on the loss tangent  $\tan \delta$  (eq 3) which by definition does not depend on geometry and is closely related to the imaginary part  $\epsilon''$  because the variation of  $\epsilon'$  does not exceed 13% in all of the experiments performed in this study. On the other hand, we defined a normalized real part of permittivity  $\epsilon'_n$  by dividing  $\epsilon'(\omega)$  by its value measured at 400 Hz:

$$\epsilon'_n(\omega) = \frac{\epsilon'(\omega)}{\epsilon'(\omega = 400 \text{ Hz})} \quad (7)$$

As geometric effects are independent of frequency,  $\epsilon'_n(\omega)$  is not influenced by these effects. Thus, we used  $\epsilon'_n(\omega)$  in order to have a good comparison between the dielectric measurements performed during a temperature increase and those performed during a sample deformation.

### 3. RESULTS

**3.1. Temperature Response.** Before investigating the effect of the uniaxial deformation on the dielectric response, we want to discuss the temperature dependence of PC dielectric properties. An important key is to test whether a strain energy modifies the molecular dynamics in the same way as the thermal one. We measured the dielectric response of the PC films at rest as a function of temperature, from room temperature up to  $T_g + 20$  K (443 K). For these measurements we used a film sample of 40 mm in diameter. Figure 2 shows

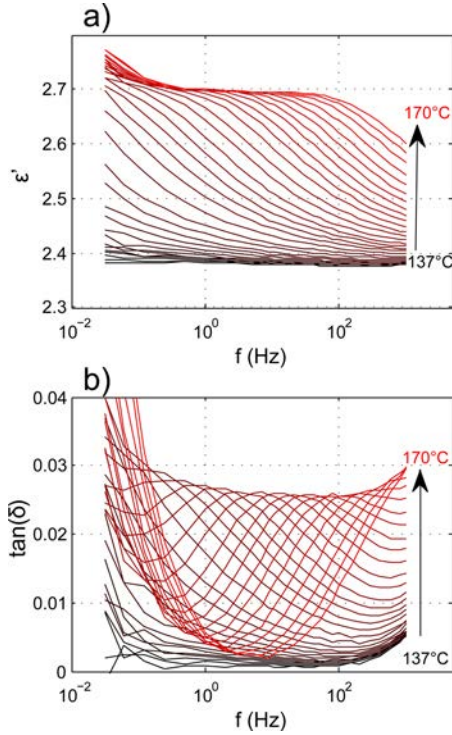


**Figure 2.** Dielectric permittivity as a function of frequency in a temperature range from  $T_g - 13$  to  $T_g + 20$ : (a) real part and (b)  $\tan \delta$ . The temperature increment between two curves is 1 K.

the evolution of  $\epsilon'(\omega)$  and  $\tan \delta(\omega)$  as a function of temperature from  $T_g - 13$  K up to  $T_g + 20$  K.  $\epsilon'(\omega)$  increases with temperature. Near  $T_g$ , it forms a sigmoid curve in our measurement frequency window. This evolution of  $\epsilon'(\omega)$  corresponds to the shift of the  $\alpha$ -relaxation. Upon increasing the temperature,  $\tan \delta(\omega)$  increases first at low frequency, until a peak appears in our frequency window. This peak and its shift toward high frequencies are also a well-known signature of the  $\alpha$ -relaxation activation. Note that the further increase at low frequency corresponds to conduction. Taking advantage of the temperature–frequency equivalence,  $\epsilon'(\omega)$  and  $\tan \delta(\omega)$  obtained at different temperatures around  $T_g$  collapse on two master curves presented in Figure 3. The deviations from superimposition that one can observe at low frequency are due to conduction. The master curves were obtained by rescaling frequencies according to the Vogel–Fulcher–Tammann equation for the  $\alpha$ -relaxation frequency:

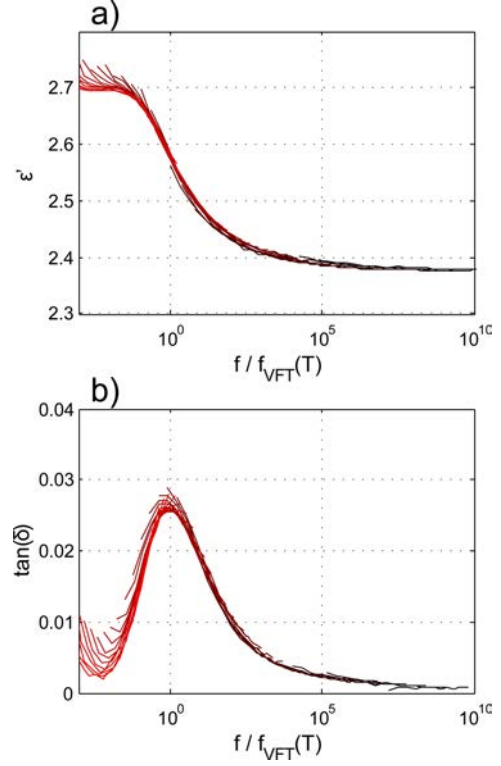


**Figure 3.** Real part of the permittivity  $\epsilon'$  (a) and  $\tan \delta$  (b) in a temperature range from  $T_g - 13$  K to  $T_g + 20$  K as a function of frequency scaled according to Vogel–Fulcher equation with  $T_{VFT} = T_g - 43$  K,  $D_{VFT} = 3.9$ , and  $f_0 = 1.7 \times 10^{13}$  Hz.

$$f_{VFT}(T) = f_0 \exp\left(\frac{D_{VFT} T_{VFT}}{T_{VFT} - T}\right) \quad (8)$$

with the parameters of the VFT equation  $T_{VFT} = T_g - 43$  K,  $D_{VFT} = 3.9$ , and  $f_0 = 1.7 \times 10^{13}$  Hz. These values are in good agreement with previous measurements on PC (see ref 46).

### 3.2. Dielectric Response under Uniaxial Deformation.

The dielectric response of PC was then measured during uniaxial deformation. Figure 4 presents the force-stretching profiles for different strain rates:  $2.5 \times 10^{-3} \text{ s}^{-1}$ ,  $2.5 \times 10^{-4} \text{ s}^{-1}$ ,  $2.5 \times 10^{-5} \text{ s}^{-1}$ , and  $2.5 \times 10^{-6} \text{ s}^{-1}$ . The samples were stretched up to 8% deformation. The curves present the well-known maximum on stress called yield stress which is at about 6% of

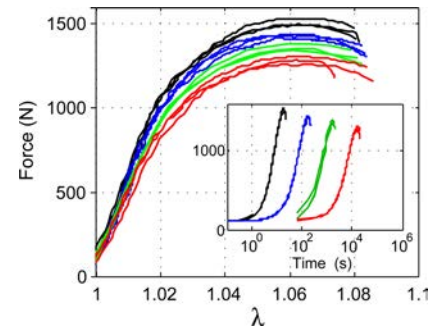


**Figure 4.** Force in newtons as a function of  $\lambda$  for stretching experiments at  $2.5 \times 10^{-3}$ ,  $2.5 \times 10^{-4}$ ,  $2.5 \times 10^{-5}$ , and  $2.5 \times 10^{-6} \text{ s}^{-1}$ . The inset represents the force as a function of time (time in logarithmic scale) for the same experiments. Several identical specimens have been measured for each strain rate.

deformation ( $\lambda = 1.06$ ). As mentioned above, we focused our study in the range from zero to the yield stress.

In the linear regime, the stress is independent of the strain rate. The stress level starts to show some measurable dependence on the strain rate at a strain value of order 0.01.

In order to emphasize the time scale explored with these deformation experiments, the inset in Figure 4 presents the measured stress over time on a semilogarithmic scale. Qualitatively, the maximum stress increases as the logarithm of the strain rate, which is in agreement with previous mechanical studies of PC (see ref 47).

Figure 5 shows  $\epsilon'_n$  (defined above) and the loss tangent  $\tan \delta$  as a function of frequency during uniaxial stretching for a strain

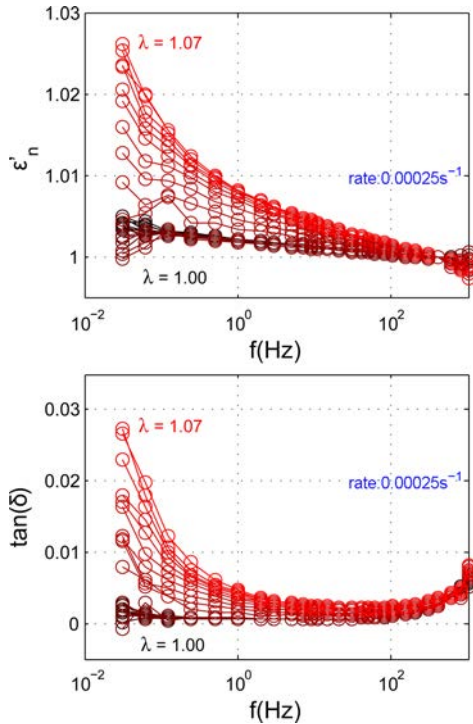


**Figure 5.** Normalized real part  $\epsilon'_n$  (see section 2.5) and  $\tan \delta$  as a function of frequency during the uniaxial stretching at  $2.5 \times 10^{-4} \text{ s}^{-1}$ : from  $\lambda = 1$  (black) and  $\lambda = 1.07$  (red). The strain increment between each curve is 0.008.

rate of  $2.5 \times 10^{-4} \text{ s}^{-1}$  up to a 7% deformation. There is a large increase of  $\epsilon'_n$  at low frequencies. This increase of the real component of permittivity is the signature of the strain induced  $\alpha$ -relaxation that takes place during plastic deformation. The loss tangent,  $\tan \delta$ , increases at low frequencies also. We observe almost no change in  $\tan \delta$  at high frequencies. The shift of  $\alpha$ -relaxation toward higher frequencies during deformation is in agreement with the recent work of Kalfus et al.<sup>28</sup> on PVC. These results are also consistent with the measurements performed by Ediger's group with molecular fluorescent probes.<sup>48</sup> In our study, measurements were performed at temperature  $T_g - 125 \text{ K}$ , while previous study were performed closer to  $T_g$ : Kalfus et al.<sup>28</sup> were working at  $T_g - 50 \text{ K}$  with PVC, and Ediger was working at temperatures higher than  $T_g - 20 \text{ K}$ .

The modification of the dielectric response during deformation can be observed in a different way in Figure 6, where we plot  $\epsilon'_n$  as a function of the stretching ratio for five different frequencies and  $\tan \delta$  normalized to its value before

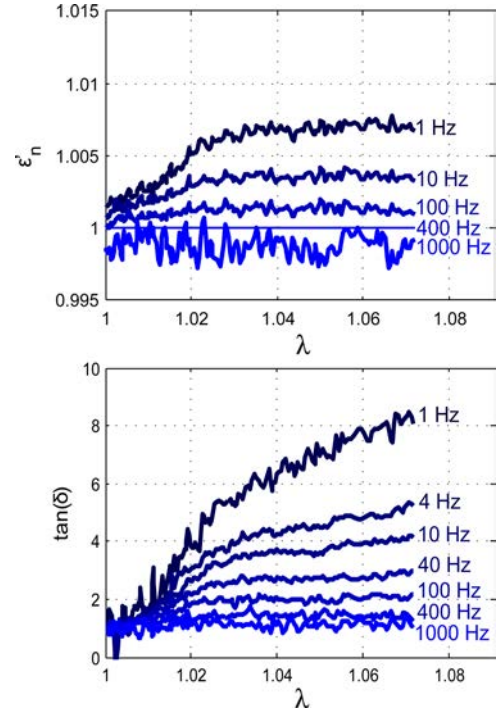


**Figure 6.** Normalized real part  $\epsilon'_n$  (see section 2.5) and  $\tan \delta$  normalized by its initial value as a function of  $\lambda$  at different frequencies for a stretching experiment at  $2.5 \times 10^{-4} \text{ s}^{-1}$ .

stretching,  $\tan \delta(\lambda)/\tan \delta(\lambda=1)$ . The results indicate the importance of characterizing the  $\alpha$ -relaxation during the different deformation stages in order to understand the plastification phenomenon.

One can observe an increase of the dielectric response at all frequencies, even at very small deformation. The increase is more marked around 1% deformation and beyond. The small increase of the dielectric response might be the signature that the distribution of the relaxation time is either shifted by many decades or at least deformed in its high frequency part. More specifically, this means that even at very small strain the high frequency part of this spectrum enters in the frequency window of our experiment. The change of the distribution of relaxation times as compared to the sample at rest, which may be observed here at deformations of a few 0.1%, would then correspond to nonlinear effects, due to significant changes of internal free energy barrier under the applied strain, even before the onset of plastic flow at a few percent of deformation.

The latter value is in agreement with experiments by the observation of shear bands in PC by Lu and Ravi-Chandar<sup>49</sup> and also with experiments performed on thin films by Liu et al.<sup>50</sup> Note that this level of deformation (1%) corresponds to the point at which the stress starts to show a dependence on the strain rate (Figure 4). Unexpectedly, the real part and the loss tangent seems to reach a plateau near 4% deformation. This plateau between 4% and 7% deformation is in contrast with the well-known maximum stress reached at 6% deformation (see Figure 4). This result underlines that the relation between macroscopic behaviors (stress–deformation) and microscopic mechanisms is nontrivial: the dielectric signal reaches a plateau whereas the stress displays a nonmonotonic behavior.

**3.3. Strain Rate Effect.** The effect of strain rate was explored by performing measurements at four different strain

rates:  $2.5 \times 10^{-3}$ ,  $2.5 \times 10^{-4}$ ,  $2.5 \times 10^{-5}$ , and  $2.5 \times 10^{-6} \text{ s}^{-1}$ . In Figure 7, the variation of the normalized real part of the

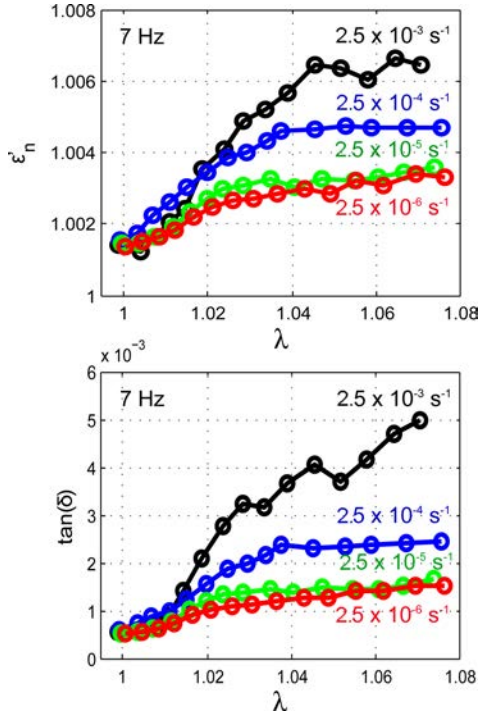


**Figure 7.** Strain rates effect on (a) the normalized real part  $\epsilon'_n$  and (b)  $\tan \delta$  (normalized by its initial value) measured at frequency  $f = 7 \text{ Hz}$  as a function of  $\lambda$ . Strain rates are  $2.5 \times 10^{-3}$ ,  $2.5 \times 10^{-4}$ ,  $2.5 \times 10^{-5}$ , and  $2.5 \times 10^{-6} \text{ s}^{-1}$ . Each curve is obtained by averaging the results of three measurements.

permittivity  $\epsilon'_n$  and the loss tangent  $\tan \delta$  at 7 Hz are represented as a function of  $\lambda$  for the four different strain rates. The comparison is shown at 7 Hz because it is the frequency at which dielectric properties can be determined with good signal-to-noise ratio for all applied strain rates (see section 2.5). Both components of the permittivity increase with the strain rate. The molecular mobility ( $\alpha$ -relaxation) increases with the deformation rate. The onset of the molecular mobility increase is at 1% deformation for all strain rates.

**3.4. Glass Transition and Plastic Deformation.** The dielectric measurements on PC under deformation presented above reveal the increased mobility of polymer segments in the frequency range between 0.03 and 100 Hz. This mobility is related to the  $\alpha$ -relaxation. The  $\alpha$ -relaxation is active in this frequency range near the glass transition. Therefore, the dielectric measurements obtained under deformation at different strain rates were compared to data obtained when heating up a sample through the glass transition ( $T_g = 423 \text{ K}$ ) without stretching it.

**3.4.1. Equivalent Temperature.** In Figure 8,  $\epsilon'_n(\omega)$  and  $\tan \delta(\omega)$ , measured at 7% deformation ( $\lambda = 1.07$ ) and at four strain rates, are compared to the measurements close to  $T_g$  without deformation. It can be observed that  $\epsilon'_n(\omega)$  superimposes quite well with the dielectric response at temperatures close to  $T_g$ , where the considered temperatures depend on the strain rate. The comparison suggests that the sample under deformation at room temperature behaves like PC close to  $T_g$ . Thus, we may introduce an apparent temperature of the sample under deformation depending on the strain rate,  $T_a(\dot{\gamma}, \lambda)$ : 146 °C

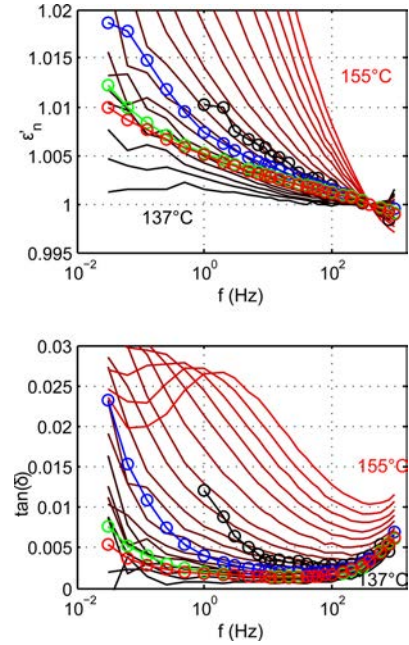


**Figure 8.** Normalized real part of the permittivity  $\epsilon'_n$  (a) and  $\tan \delta$  (b) measured under deformation at  $\lambda = 1.07$  as a function of frequency (lines with circles) at strain rates (from top to bottom):  $2.5 \times 10^{-3} \text{ s}^{-1}$  (black),  $2.5 \times 10^{-4} \text{ s}^{-1}$  (blue),  $2.5 \times 10^{-5} \text{ s}^{-1}$  (green), and  $2.5 \times 10^{-6} \text{ s}^{-1}$  (red). They can be compared to equivalent measurements without deformation at temperatures from 137 to 155 °C (simple lines, 1 °C increment between curves).

for  $2.5 \times 10^{-3} \text{ s}^{-1}$ , 144 °C for  $2.5 \times 10^{-4} \text{ s}^{-1}$ , and 141 °C for  $2.5 \times 10^{-5}$  and  $2.5 \times 10^{-6} \text{ s}^{-1}$ .

Correspondingly, the loss tangent,  $\tan \delta(\omega)$ , at 7% deformation (Figure 8b) is found close to  $\tan \delta(\omega)$  measured at temperatures close to  $T_g$  without stretching. However, the curves do not superimpose as well as  $\epsilon'$  to  $\tan \delta(\omega)$ . The rise at low frequencies is steeper as compared to the rise at low frequencies of the unstrained samples measured at temperatures close to  $T_g$ . At the moment, we do not have a definitive explanation for that since we do not measure the whole distribution of relaxation times. Two different effects may explain this. A first explanation may be that this is due to conductivity effects: at room temperature, our samples may contain impurities of amount slightly larger than at temperatures close to  $T_g$ . Another possibility is that the distribution of relaxation times of the sample at room temperature is narrower upon stretching as compared to the sample at rest at 146 °C, as it has been observed by Ediger et al.<sup>26</sup> when comparing the distribution of relaxation times at rest and upon stretching at the same temperature.

Note that polycarbonate exhibits various relaxation mechanisms which have been studied by Yee.<sup>51</sup> The temperature  $T_\beta$  associated with the  $\beta$ -relaxation of polycarbonate is 80 °C (see Figure 2 in ref 51), which is much lower than  $T_g$ . Because of this big temperature difference between  $T_\beta$  and  $T_g$ , it is conceivable that the  $\beta$ -relaxation has a negligible effect on the dielectric properties measured in the vicinity of  $T_g$ . Furthermore, the temperature  $T_\beta$  is much higher than room temperature at which our dielectric measurements under strain have been performed. Thus, we do not expect significant contribution of the  $\beta$ -relaxation on our results. The  $\gamma$ -relaxation of the polymer does not interfere much with our experiment since  $T_\gamma = -100 \text{ °C}$ .

**3.4.2. Mobile Fraction.** We aim at comparing the dielectric relaxation under stress to the dielectric relaxation of the same material at rest at higher temperature. The idea is that some part of the sample becomes mobile under the applied deformation. The question which arises is the following: Does the whole sample become mobile, or only a part of it? The last would be the case if the macroscopic strain was localized on small scales as for instance in the shear bands. In such a case, only a fraction of the material would become mobile, and this accelerated fraction would coexist with the other slow and glassy parts of the material. The latter would not contribute to the dielectric signal in the frequency domain to which we have access and the effective amplitude of the dielectric response would be smaller than the one measured by increasing temperature toward  $T_g$ .

The opposite situation without the presence of localization (shear bands) corresponds to an homogeneous deformation of the sample; i.e., the whole sample is rejuvenated by the mechanical stress. In such a case, one expects a shift of the whole distribution of relaxation times. Stochastic models have been developed for studying the evolution of the relaxation time spectrum during cooling and heating<sup>52</sup> and also under applied strain.<sup>53</sup> These authors predict a shift of the relaxation time spectrum toward higher frequencies under strain similar to the evolution upon heating. The results reported here are qualitatively consistent with these models. The issue is then: can we discriminate between homogeneous deformation and shear bands by comparing the dielectric spectrum and its amplitude under strain to the dielectric spectrum and its amplitude at a higher temperature? This comparison is delicate because we have no access to the whole dielectric spectrum since our experimental setup covers only 4–5 decades in frequency. In addition, we cannot measure in the transient regime of deformation frequencies smaller than  $1/t$ , where  $t$  is the duration of the experiment.

$\epsilon'(\omega)$  is related to the amount of mobile polymer segments. Then, the change of  $\epsilon'(\omega, \lambda)$  from 0 to 7% deformation could be interpreted as an increase of the mobile fraction within the material. This requires to recover some meaningful  $\epsilon'(\omega)$  from the normalized  $\epsilon'_n(\omega)$ . Interestingly, according to the definition of  $\epsilon'_n(\omega)$ , we simply need to restore the variation of the real component of permittivity at 400 Hz:

$$\epsilon'(\omega, \lambda) = \epsilon'_n(\omega, \lambda) \epsilon'(400 \text{ Hz}, \lambda) \quad (9)$$

Taking advantage of the equivalence found between plastic deformation and heating through the glass transition,  $\epsilon'$  at 400 Hz under deformation was assimilated to  $\epsilon'$  at 400 Hz without stretching at the apparent temperature,  $T_a(\dot{\gamma})$ , defined in the previous paragraph:

$$\epsilon'(400 \text{ Hz}, \lambda) \sim \epsilon'(400 \text{ Hz}, T = T_a(\dot{\gamma}, \lambda)) \quad (10)$$

Then, this reconstructed  $\epsilon'(\omega)$  measured under constant strain rate deformation can be superimposed on  $\epsilon'(\omega)$  curves measured close to  $T_g$  without stretching. These data are found to be remarkably similar (see Figure 9). We do not have to rescale the amplitude of the dielectric signal in order to fit the dielectric response obtained at high temperature on the sample at rest. This tends to indicate that the whole sample is rejuvenated. Note that the measurement is an average over the electrode surface and that the maximal variation of the dielectric properties through rejuvenation is limited. Therefore, the contribution of a small fraction of the material, e.g. shear bands, is probably not detectable. Strong heterogeneities, which

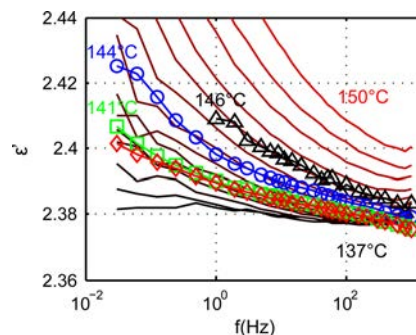


**Figure 9.** Real part of the permittivity  $\epsilon'$  (see text) measured under deformation (line with symbols) at  $\lambda = 1.07$  as a function of frequency at strain rates  $2.5 \times 10^{-3} \text{ s}^{-1}$  (black triangles),  $2.5 \times 10^{-4} \text{ s}^{-1}$  (blue circles),  $2.5 \times 10^{-5} \text{ s}^{-1}$  (green squares), and  $2.5 \times 10^{-6} \text{ s}^{-1}$  (red diamonds). Real parts of the permittivity for sample at rest at temperatures from 137 to 150 °C (simple lines) were represented as a function of frequency.

we cannot detect, may coexist with the average rejuvenation, which we are able to measure. In any case, our results support the idea that there is a relation between the glass transition and the plastic deformation. The temperature shift is consistent with the strain rate of the applied deformation as will be discussed in the next subsection.

**3.4.3. Strain Rates and Vogel Fulcher Tamman.** The good agreement between the permittivity at temperatures close to  $T_g$  (at rest) and the permittivity at 7% deformation for various strain rates (at room temperature) seen in Figure 9 reinforces the idea of an apparent temperature  $T_a(\dot{\gamma})$ . This relation can be further tested by calculating the frequencies associated with these apparent temperatures,  $f_{\text{VFT}}(T_a(\dot{\gamma}))$  at rest, from the Vogel–Fulcher–Tammann equation (see Figure 3). The results are reported in Table 1.

**Table 1.** For the Strain Rates Applied for Deformation Experiments (Left), the Apparent Temperatures at 9% Deformation (Middle), and the Associated Frequency Bounds (Right) Which Are Estimated Using the Vogel–Fulcher–Tammann Equation, Including Uncertainties on the Apparent Temperature and on the VFT Parameters

$\dot{\gamma} \text{ (s}^{-1}\text{)}$	$T_a(\dot{\gamma}) \text{ (}^\circ\text{C)}$	$f_{\text{VFT}}(T_a) \text{ (s}^{-1}\text{)}$
$2.5 \times 10^{-3}$	$146 \pm 1$	$1 \times 10^{-3} > f > 1 \times 10^{-4}$
$2.5 \times 10^{-4}$	$144 \pm 1$	$1 \times 10^{-4} > f > 1 \times 10^{-5}$
$2.5 \times 10^{-5}$	$141 \pm 1$	$4 \times 10^{-6} > f > 3 \times 10^{-7}$

Interestingly, the calculated frequencies are lower but close to the strain rates, which leads to the idea that during deformation the  $\alpha$ -relaxation is simply forced to be close to the strain rate as the sample reaches the yield point, or even a little bit below the yield point (when it reaches a plateau in  $\epsilon'$ , see Figure 6), despite the sample is 125 K below its glass transition temperature. The frequencies associated with the apparent temperatures are lower than the strain rates by about roughly 1 decade or so. This result suggests that the mechanical stress does not simply impose the  $\alpha$ -relaxation time because some aging occurs along with strain or stress induced rejuvenation. This interpretation is consistent with theoretical results by Chen and Schweizer<sup>54</sup> and experimental results by Hebert et al.<sup>48</sup> Note that these two groups have shown that the dominant relaxation time during plastic flow increases upon cooling,

though in a very different and much smaller way as compared to the VFT law of the undeformed polymer. The dominant relaxation time is not set uniquely by the strain rate and is thus a function both of the strain rate and of temperature. Note also that the model of Chen and Schweizer<sup>54</sup> indicates that the dominant relaxation time  $\tau_\alpha$  varies roughly like  $\dot{\gamma}^{-0.8}$  during plastic flow, consistent with the experiments by Hebert et al.<sup>48</sup>

As the strain rate is smaller, the material has more time to age during the tensile test, which explains the dependence on the strain rate and the strong correlation between the estimated frequency  $f_{\text{VFT}}(T_a(\dot{\gamma}))$  and the strain rate (as illustrated in Table 1). Increasing aging at lower strain rate also corresponds to increasing stress relaxation, which explains the increase of the maximum stress as the strain rate increases (as shown in Figure 4).

#### 4. DISCUSSION

We have measured the dielectric response of polycarbonate under applied strain in the frequency domain from  $10^{-2}$  Hz up to  $10^3$  Hz. Our main observations are the following. The dynamics is accelerated under the applied strain. This acceleration of the dynamics can be observed in Figure 5, for instance. We see that the dielectric response is amplified in the low frequency range of our accessible window, between  $10^{-2}$  Hz and a few Hz. It is observed that the dielectric response at frequencies higher than a few Hz is not modified as compared to that of the unstretched samples. The second important observation is that the dielectric response at room temperature under stress can be compared to the dielectric response of the unstretched samples at much higher temperature.

It can be seen in Figure 9 that the dielectric response at strain rate  $\dot{\gamma}$  and at the yield point superimposes to that at  $T_a(\dot{\gamma}) < T_g$  where  $T_a$  is consistent with the strain rate and the time scale set for defining the glass transition temperature, which is  $\dot{\gamma}^{-1} \sim \tau_\alpha(T_a)$ . The accessible frequency domain of our experimental setup does not allow us to cover the full frequency range of the relaxation spectrum of the stretched sample. The interpretation we propose is the following one (see Figure 10). At room temperature, the distribution of relaxation times of the unstretched sample looks like curve (1).<sup>a</sup> As a consequence of the applied deformation, the distribution of relaxation times shifts toward shorter times (higher frequencies), curve (2). Only the high frequency part of the spectrum is accessible to our setup. Note that in Figure 10 the curves are only schematic. In particular, the curve at 300 K would represent the relaxation time spectrum of a sample below  $T_g$  which would have aged for a few days. If aged for a longer time, the curve would shift farther to the left, at lower frequencies.

The relaxation time distribution which is schematized by curve (2) corresponds to a steady state regime, at least in the deformation range that we consider, i.e., at and beyond the yield point. Two different processes compete during the deformation: the applied strain tends to accelerate the dynamics (rejuvenation), and an aging process tends to shift back the spectrum toward the spectrum at rest, i.e., toward lower frequencies, or, in other words, to suppress the high frequency part of the spectrum, as has been discussed by Chen and Schweizer.<sup>54</sup>

This phenomenon has been described phenomenologically by Eyring in the context of a mean field picture, with only a single relaxation time. In the context of the heterogeneous nature of the dynamics, one may assume that slow subunits melt and acquire a fast relaxation time as a result of the local

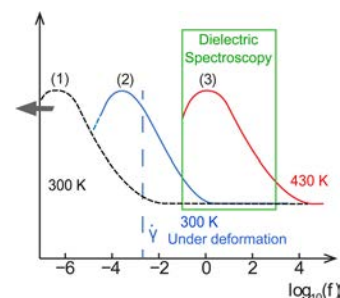


**Figure 10.** Schematics of rejuvenation under uniaxial strain of polycarbonate. The black curve represents the relaxation spectrum (in frequency) of PC at room temperature. Note that well below  $T_g$  the polymer undergoes an aging process during which the distribution of relaxation times shifts progressively toward low frequencies. Here the black dashed curve represents qualitatively a distribution after a few days of aging. The lowest frequency corresponds to the inverse of the aging time of the sample below  $T_g$ . The red curve corresponds to the dielectric spectrum of the sample at rest at 430 K. The blue curve corresponds to the spectrum of the stretched sample at room temperature. The spectrum corresponds to that of the glassy sample at rest shifted toward higher frequencies. The dielectric spectrum of the strained sample is not modified as compared to the one at rest in the high frequency domain (i.e., at frequencies higher than 10 Hz). Differences between the two spectrum cannot be properly established with our data and are not represented. The spectrum of the strained sample results from two competing processes: a rejuvenating process due to the applied strain and an aging process which tends to suppress the high frequency part of the spectrum.

stress. The rejuvenated sample ages because the temperature is much lower than the glass transition temperature  $T_g$  of PC. In particular, the fast relaxation times acquired by relaxed subunits age faster than slow times. When working far below  $T_g$ , we cannot access the possibly very fast relaxation times generated instantaneously by deformation: indeed, we observe no changes of the relaxation time spectrum for frequencies larger than 10 Hz. It would be interesting to perform the same experiments at higher temperature and measure the high frequency cutoff in the spectrum: possibly it may differ as compared to the one (10 Hz) measured in our experiment.

In order to give new insight into this problem, it would be interesting to repeat the experiment at higher temperatures in such a way that for the same strain rate and experimental duration one could have access to different parts of the relaxation spectrum. Indeed, one has not to forget that this experiment measures transient effects. The frequency is thus limited by the duration of the experiment. This study will be made feasible thanks to the ongoing development of our current setup for working at temperatures higher than room temperature. In particular, it would allow for answering the question whether the spectrum is shifted to higher frequency even at very small deformation as is suggested by Chen and Schweizer theory<sup>54</sup> and by Ediger et al.<sup>26</sup> experiments using optical probes. Note that the results in Figure 6 suggest that the dynamics progressively accelerates even at very small strain.

Thus, we observe that the dielectric relaxation  $\epsilon'(\omega)$  under strain at room temperature fits the dielectric spectrum of the undeformed sample at a temperature just below  $T_g$ . The fit is obtained without a prefactor. A prefactor would be required if the deformation was localized in shear bands (because only a fraction of the material would be deformed) or if the width of the distribution of relaxation times was very different under strain to the one we compare with. Ediger and co-workers have



considered this issue by studying reorientation dynamics of optical probes. They observed that the distribution of relaxation times of the sample under strain is narrower as compared to that of the sample at rest at the same temperature. Here we compare the relaxation time spectrum (for the accessible window) between the strain sample at room temperature and that of the unstrained sample slightly below  $T_g$ , which is at temperatures close to 150 °C. Within the experimental uncertainty, we observe that the relaxation time spectrum of the strained sample in the plastic regime at room temperature when measured with  $\varepsilon'$  is similar to that of the same polymer at rest at 146 °C. On the other hand, when considering  $\tan \delta$ , we observe a sharper increase at low frequencies in the case of the stretched sample as compared to the unstretched one at higher temperature we compared with. We cannot rule out that the relaxation time spectrum is narrower under strain at room temperature as compared to the unstretched samples at 146 °C. It may be also due to the fact that at room temperature our samples may contain impurities of amount slightly larger than at temperatures close to  $T_g$ . We cannot compare the width of the relaxation time spectrum under strain to the one at rest at the same temperature because the latter is not accessible to our apparatus and as regard also to the transient nature of our experiment. For making this comparison, one would need to perform this experiment at a higher temperature, typically at  $T_g - 10-20$  K for which the relaxation times distribution would be at least partially accessible. Our apparatus does not allow us to currently perform such measurements. Work is in progress in order to modify the experimental setup for making experiments at temperatures closer to  $T_g$  than the present ones.

## 5. CONCLUSION

We have studied the dielectric relaxation of polycarbonate under applied strain at a temperature much below the glass transition of PC (about 125 K below  $T_g$ ). We have shown that the relaxation spectrum fits on the relaxation spectrum of the unstretched polymer measured at a temperature slightly below  $T_g$ . The temperature shift is a function of the applied strain rate; thus, we obtain a temperature/strain rate superposition result. Our results are consistent with the fact that the whole sample is deformed and rejuvenated. However, heterogeneities and strain localizations, such as shear bands, are part of the average effect we measured. The heterogeneity contributions cannot be really separated because the frequency range for which we can measure the relaxation spectrum is limited and the intrinsic amplitude of dielectric permittivity variations is small, as compared to mechanical moduli. The development of local dielectric measurements may bring complementary information.

## AUTHOR INFORMATION

### Corresponding Authors

\*E-mail: didier.long-exterieur@solvay.com (D.R.L.).

\*E-mail: sergio.ciliberto@ens-lyon.fr (S.C.).

### Notes

The authors declare no competing financial interest.

## ACKNOWLEDGMENTS

R. Pérez-Aparicio and D. Cottinet acknowledge the funding by Solvay. We thank Marius Tanase for the help with the electronics part and Frédéric Arnould for the design and manufacture of the tensile machine. We also thank Stephane

Santucci for the fruitful discussions and preliminary measurements.

## ADDITIONAL NOTE

<sup>a</sup>Note that we cannot probe experimentally the distribution of relaxation times of the sample at rest at room temperature. Struik has studied aging in his classical book.<sup>55</sup> He has studied in particular the compliance  $J(t, t_w)$  which is a function of time  $t$  measured after the sample has aged for a time  $t_w$  at a temperature  $T$  lower than  $T_g$ . He has shown that the compliance collapses on a master curve  $J(t, t_w) = J(t/t_w^\mu)$ , where  $\mu$  is an exponent close to 1. The interpretation of his experiments is that the dominant relaxation time  $\tau_\alpha$  evolves with the aging time  $t_w$  like  $\tau_\alpha \propto t_w^\mu \approx t_w$ . In particular, as long as the aging process lasts, which is for all accessible waiting times at temperatures well below  $T_g$ ,  $\tau_\alpha$  is not sensitive to the temperature, but only to the waiting time. Note that this point of view has been described theoretically by Merabia and Long in ref 52. We assume that the curve (1) in Figure 10 corresponds to an aging time of e.g.  $10^6$  s. Since we cannot probe this distribution, we plotted the schematic curve (1) as a dotted line.

## REFERENCES

- (1) Ferry, J. D. *Viscoelastic Properties of Polymers*; John Wiley and Sons, Inc.: New York, 1980.
- (2) Doi, M., Edwards, S. F. *The Theory of Polymer Dynamics*; Oxford University Press: New York, 1988.
- (3) Richter, R.; Monkenbusch, M.; Arbe, A.; Colmenero, J. *Neutron Spin Echo in Polymer Systems*; Springer-Verlag: Berlin, 2005; Adv. Polym. Sci. Vol. 174.
- (4) Binder, K. *Monte Carlo and Molecular Dynamics Simulations in Polymer Science*; Oxford University Press: Oxford, 1995.
- (5) Götze, W. In *Liquids, Freezing, Glass Transition*; Hansen, J. P., Levesque, D., Zinn-Justin, J., Eds.; North-Holland: Amsterdam, 1991; p 287.
- (6) Pérez-Aparicio, R.; Arbe, A.; Alvarez, F.; Colmenero, J.; Willner, L. Quasielastic neutron scattering and molecular dynamics simulation study on the structure factor of poly(ethylene-alt-propylene). *Macromolecules* **2009**, *42*, 8271–8285.
- (7) Ediger, M. D. Spatially heterogeneous dynamics in supercooled liquids. *Annu. Rev. Phys. Chem.* **2000**, *51*, 99–128.
- (8) Richert, R. Heterogeneous dynamics in liquids: fluctuations in space and time. *J. Phys.: Condens. Matter* **2002**, *14*, R703–R738.
- (9) Schmidt-Rohr, K.; Spiess, H. W. Nature of nonexponential loss of correlation above the glass-transition investigated by multidimensional nmr. *Phys. Rev. Lett.* **1991**, *66*, 3020–3023.
- (10) Tracht, U.; Wilhelm, M.; Heuer, A.; Feng, H.; Schmidt-Rohr, K.; Spiess, H. W. Length scale of dynamic heterogeneities at the glass transition determined by multidimensional nuclear magnetic resonance. *Phys. Rev. Lett.* **1998**, *81*, 2727–2730.
- (11) Reinsberg, S. A.; Qiu, X. H.; Wilhelm, M.; Spiess, H. W.; Ediger, M. D. Length scale of dynamic heterogeneity in supercooled glycerol near  $T_g$ . *J. Chem. Phys.* **2001**, *114*, 7299–7302.
- (12) Cicerone, M. T.; Blackburn, F. R.; Ediger, M. D. Anomalous diffusion of probe molecules in polystyrene evidence for spatially heterogeneous segmental dynamics. *Macromolecules* **1995**, *28*, 8224–8232.
- (13) Cicerone, M. T.; Wagner, P. A.; Ediger, M. D. Translational diffusion on heterogeneous lattices: A model for dynamics in glass forming materials. *J. Phys. Chem. B* **1997**, *101*, 8727–8734.
- (14) Wang, C.-Y.; Ediger, M. D. Enhanced translational diffusion of 9,10-bis(phenylethynyl)anthracene (bpea) in polystyrene. *Macromolecules* **1997**, *30*, 4770–4771.

- (15) Fujara, F.; Geil, B.; Sillescu, H.; Fleischer, G. Translational and rotational diffusion in supercooled orthoterphenyl close to the glass transition. *Z. Phys. B: Condens. Matter* **1992**, *88*, 195–204.
- (16) Hwang, Y.; Inoue, T.; Wagner, P. A.; Ediger, M. D. Molecular motion during physical aging in polystyrene: Investigation using probe reorientation. *J. Polym. Sci., Part B: Polym. Phys.* **2000**, *38*, 68–79.
- (17) Schiener, B.; Böhmer, R.; Loidl, A.; Chamberlin, R. V. Nonresonant spectral hole burning in the slow dielectric response of supercooled liquids. *Science* **1996**, *274*, 752–754.
- (18) Richert, R. Triplet state solvation dynamics: Basics and applications. *J. Chem. Phys.* **2000**, *113*, 8404–8229.
- (19) Crauste-Thibierge, C.; Brun, C.; Ladieu, F.; L'Hôte, D.; Biroli, G.; Bouchaud, J.-P. Evidence of growing spatial correlations at the glass transition from nonlinear response experiments. *Phys. Rev. Lett.* **2010**, *104*, 165703.
- (20) Nielsen, L. E.; Landel, R. F. *Mechanical Properties of Polymers and Composites*; Marcel Dekker: New York, 1994.
- (21) McKenna, G. B. Mechanical rejuvenation in polymer glasses: fact or fallacy? *J. Phys.: Condens. Matter* **2003**, *15* (11), S737–S763.
- (22) Meijer, H. E. H.; Govaert, L. E. Multi-scale analysis of mechanical properties of amorphous polymer systems. *Macromol. Chem. Phys.* **2003**, *204* (2), 274–288.
- (23) Chen, K.; Schweizer, K. S. Stress-enhanced mobility and dynamic yielding in polymer glasses. *Europhys. Lett.* **2007**, *79* (2), 26006.
- (24) Chen, K.; Schweizer, K. S. Microscopic constitutive equation theory for the nonlinear mechanical response of polymer glasses. *Macromolecules* **2008**, *41* (15), 5908–5918.
- (25) Loo, L. S.; Cohen, R. E.; Gleason, K. K. Chain mobility in the amorphous region of nylon 6 observed under active uniaxial deformation. *Science* **2000**, *288*, 116–119.
- (26) Lee, H.-N.; Paeng, K.; Swallen, S. F.; Ediger, M. D. Direct measurement of molecular mobility in actively deformed polymer glasses. *Science* **2009**, *323*, 231–234.
- (27) Bending, B.; Christison, K.; Ricci, J.; Ediger, M. D. Measurement of segmental mobility during constant strain rate deformation of a poly(methyl methacrylate) glass. *Macromolecules* **2014**, *47*, 800–806.
- (28) Kalfus, J.; Detwiler, A.; Lesser, A. J. Probing segmental dynamics of polymer glasses during tensile deformation with dielectric spectroscopy. *Macromolecules* **2012**, *45*, 4839–4847.
- (29) Tsamados, M.; Tanguy, A.; Goldenberg, C.; Barrat, J.-L. Local elasticity map and plasticity in a model lennard-jones glass. *Phys. Rev. E* **2009**, *80*, 026112.
- (30) Papakonstantopoulos, G. J.; Riggleman, R. A.; Barrat, J.-L.; de Pablo, J. J. Molecular plasticity of polymeric glasses in the elastic regime. *Phys. Rev. E* **2008**, *77*, 041502.
- (31) Riggleman, R. A.; Schweizer, K. S.; de Pablo, J. J. Nonlinear creep in a polymer glass. *Macromolecules* **2008**, *41*, 4969–4977.
- (32) Yoshimoto, K.; Jain, T. S.; van Workum, K.; Nealey, P. F.; de Pablo, J. J. Mechanical heterogeneities in model polymer glasses at small length scales. *Phys. Rev. Lett.* **2004**, *93*, 175501.
- (33) Leonforte, F.; Boissière, R.; Tanguy, A.; Wittmer, J. P.; Barrat, J.-L. Continuum limit of amorphous elastic bodies. iii. three-dimensional systems. *Phys. Rev. B: Condens. Matter Mater. Phys.* **2005**, *72*, 224206.
- (34) Riggleman, R. A.; Lee, H.-N.; Ediger, M. D.; de Pablo, J. J. Heterogeneous dynamics during deformation of a polymer glass. *Soft Matter* **2010**, *6*, 287–291.
- (35) Riggleman, R. A.; Lee, H.-N.; Ediger, M. D.; de Pablo, J. J. Free volume and finite-size effects in a polymer glass under stress. *Phys. Rev. Lett.* **2007**, *99*, 215501.
- (36) Dequidt, A.; Long, D. R.; Sotta, P.; Sanseau, O. Mechanical properties of thin confined polymer films close to the glass transition in the linear regime of deformation: Theory and simulations. *Eur. Phys. J. E: Soft Matter Biol. Phys.* **2012**, *35*, 61.
- (37) Schweizer, K. S.; Saltzman, E. J. Entropic barriers, activated hopping, and the glass transition in colloidal suspensions. *J. Chem. Phys.* **2003**, *119*, 1181–1196.
- (38) Schweizer, K. S.; Saltzman, E. J. Theory of dynamic barriers, activated hopping, and the glass transition in polymer melts. *J. Chem. Phys.* **2004**, *121*, 1984–2000.
- (39) Chen, K.; Schweizer, K. S. Suppressed segmental relaxation as the origin of strain hardening in polymer glasses. *Phys. Rev. Lett.* **2009**, *102*, 038301.
- (40) Pérez-Aparicio, R.; Crauste-Thibierge, C.; Cottinet, D.; Tanase, M.; Metz, P.; Bellon, L.; Naert, A.; Ciliberto, S. Simultaneous and accurate measurement of the dielectric constant at many frequencies spanning a wide range. *Rev. Sci. Instrum.* **2015**, *86*, 044702.
- (41) Floudas, G.; Higgins, J. S.; Meier, G.; Kremer, F.; Fischer, E. W. Dynamics of bisphenol-a polycarbonate in the glassy and rubbery states as studied by neutron scattering and complementary techniques. *Macromolecules* **1993**, *26*, 1676–1682.
- (42) Cangialosi, D.; Schut, H.; van Veen, A.; Picken, S. J. Positron annihilation lifetime spectroscopy for measuring free volume during physical aging of polycarbonate. *Macromolecules* **2003**, *36*, 142–147.
- (43) Kremer, K.; Schonhals, A. *Broadband Dielectric Spectroscopy*; Springer-Verlag: Berlin, 2003.
- (44) Watanabe, H.; Matsumiya, Y.; Inoue, T. Rheo-dielectrics in oligomeric and polymeric fluids: a review of recent findings. *J. Phys.: Condens. Matter* **2003**, *15*, S909–S921.
- (45) Horio, K.; Uneyama, T.; Matsumiya, Y.; Masubuchi, Y.; Watanabe, H. Rheo-dielectric responses of entangled cis-polyisoprene under uniform steady shear and laos. *Macromolecules* **2014**, *47*, 246–255.
- (46) Huang, D.; McKenna, G. B. New insights into the fragility dilemma in liquids. *J. Chem. Phys.* **2001**, *114* (13), 5621–5630.
- (47) Mulliken, A. D.; Boyce, M. C. Mechanics of the rate-dependent elastic-plastic deformation of glassy polymers from low to high strain rates. *Int. J. Solids Struct.* **2006**, *43* (5), 1331–1356.
- (48) Hebert, K.; Bending, B.; Ricci, J.; Ediger, M. D. Effect of temperature on postyield segmental dynamics of poly(methyl methacrylate) glasses: Thermally activated transitions are important. *Macromolecules* **2015**, *48* (18), 6736–6744.
- (49) Lu, J.; Ravi-Chandar, K. Inelastic deformation and localization in polycarbonate under tension. *Int. J. Solids Struct.* **1999**, *36*, 391–425.
- (50) Liu, Y.; Chen, Y.-C.; Hutchens, S.; Lawrence, J.; Emrick, T.; Crosby, A. J. Directly measuring the complete stress-strain response of ultrathin polymer films. *Macromolecules* **2015**, *48*, 6534–6540.
- (51) Yee, A. F.; Smith, S. A. Molecular structure effects on the dynamic mechanical spectra of polycarbonates. *Macromolecules* **1981**, *14*, 54–64.
- (52) Merabia, S.; Long, D. Heterogeneous dynamics, ageing, and rejuvenating in van der waals liquids. *J. Chem. Phys.* **2006**, *125* (23), 234901.
- (53) Medvedev, G. A.; Caruthers, J. M. Development of a stochastic constitutive model for prediction of postyield softening in glassy polymers. *J. Rheol.* **2013**, *57*, 949–1002.
- (54) Chen, K.; Schweizer, K. S. Theory of yielding, strain softening, and steady plastic flow in polymer glasses under constant strain rate deformation. *Macromolecules* **2011**, *44*, 3988–4000.
- (55) Struik, L. *Physical Aging in Amorphous Polymers and other Materials*; Elsevier: 1978.